JBIC Journal of Biological Inorganic Chemistry (2019) 24:943–959
https://doi.org/10.1007/s00775-019-01690-1

ORIGINAL PAPER

Fabrication of the robust and recyclable tyrosinase-harboring biocatalyst using ethylenediamine functionalized superparamagnetic nanoparticles: nanocarrier characterization and immobilized enzyme properties

Kourosh Abdollahi[1,2] · Farshad Yazdani[1] · Reza Panahi[1]

Received: 23 March 2019 / Accepted: 13 July 2019 / Published online: 29 July 2019

Abstract
Immobilized tyrosinase onto the functionalized nanoparticles with the ability to be reused easily in different reaction cycles to degrade phenolic compounds is known as a substantial challenge, which can be overcome through surface modification of the particles via proper chemical groups. Herein, the synthesis and silica coating of superparamagnetic nanoparticles using a simple procedure as well as their potential for tyrosinase immobilization were demonstrated. Therefore, *N*-[3-(trimethoxysilyl)propyl]ethylenediamine was used to functionalize the silica-coated nanoparticles with amine groups. Then, the ethylenediamine functionalized magnetic nanoparticles (EMNPs) were suspended in a solution containing tetrahydrofuran and cyanuric chloride (as an activating agent) to modify nanocarriers. To immobilize enzyme, a mixture of tyrosinase and cyanuric chloride functionalized magnetic nanoparticle (Cyc/EMNPs) was shaken at room temperature. The particles were characterized by EDX, TGA, SEM, FTIR, and TEM. As a result, the successful functionalization of the magnetic nanoparticles and covalent attachment of tyrosinase onto the Cyc/EMNPs were confirmed. The fabricated nano-biocatalyst particles were semi-spherical in shape. The immobilized tyrosinase (Ty-Cyc/EMNPs) exhibited remarkable reusability of six consecutive reaction cycles while no considerable loss of activity was observed for the first three cycles. Moreover, the excellent stability of the biocatalyst at different temperatures and pHs was proved. The Ty-Cyc/EMNPs with interesting features are promising for practical applications in biosensor development and wastewater treatment.

✉ Farshad Yazdani
fyazdani@ccerci.ac.ir

[1] Chemistry and Chemical Engineering Research Center of Iran (CCERCI), P.O. Box 14335-186, Tehran, Iran

[2] School of Science, RMIT University, Bundoora West Campus, Melbourne, VIC 3083, Australia

Graphic abstract

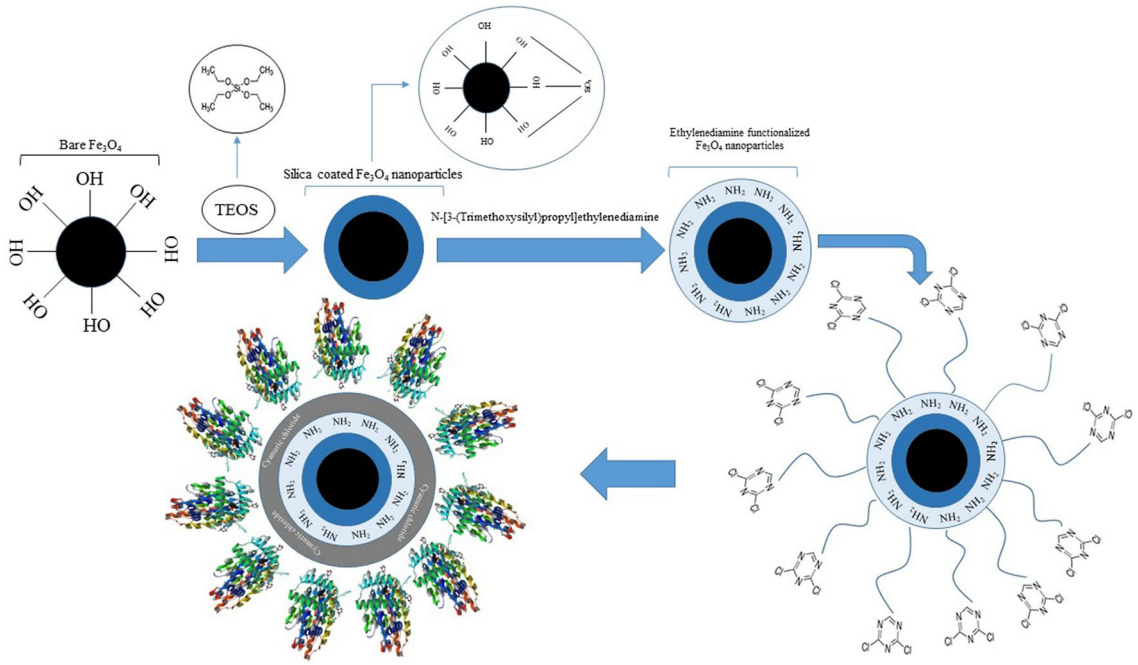

Keywords Covalent attachment · Ethylenediamine · High stability and reusability · Tyrosinase · Magnetic nanoparticles

Introduction

Enzymes are known as powerful biocatalysts offering much more competitive processes in comparison to conventional (chemical) catalysts and significantly improve the reaction rates of several chemical and biological processes [1, 2]. Recently, enzymatic bioconversion technology is considered as a "green approach" and there is a demand for robust biocatalysts [3]. In this regard, many different types of enzymes have been commercially used in various industries such as pharmaceuticals, food, textile and wastewater treatment due to their excellent properties such as high activity, enantioselectivity, and specificity towards a range of different challenging substrates [4, 5]. Stability of biocatalysts is a significant parameter for their industrial applications and they need to tolerate harsh reaction conditions such as extreme pH and high temperature [2, 3]. However, the frequent use of native or soluble enzyme in the chemical and biotechnology industries is limited due to some constraints of the free enzymes like their high sensitivity to the harsh environment, operational instability, and difficulty in reuse [6–8]. Immobilization techniques, as a powerful strategy, could overcome some of these drawbacks and enhance enzymes stability by providing efficient approaches without altering the properties of an enzyme [4]. Immobilized enzymes can be easily separated and recovered from the reaction medium which results in minimizing the contamination of the final product with the free enzyme. In addition, it is possible to reduce the cost of the relevant processes using immobilized enzymes. Some of the enzyme features such as its stability against high temperatures and various pHs and high catalytic efficiency can be greatly improved by an appropriate immobilization [9–11]. Although enzyme immobilization on different carriers can promote some advantages, negative effects due to mass transfer limitations between the substrate and enzyme, low immobilization efficiency, and the unfavorable protein conformation may also occur [11, 12]. Thus, it seems necessary to synthesize new functionalized supports for convenient and efficient immobilization which possess low biodegradability, non-toxicity, and good mechanical characteristics [4, 9]. For this reason, enormous efforts have been focused on the immobilization of biomolecules onto the different carriers. The efficient immobilization primarily relies on the preparation of a suitable chemical attachment between the carriers and enzymes. This attachment can be achieved by conventional immobilization procedures, which are divided into chemical and physical methods. The weak bonding force between the enzyme and the supporting material is one the most disadvantageous of the physical methods. This is why immobilization through the chemical methods and covalent bonding which results in increased stability of modified surfaces are mostly recommended [5, 13].

Chemically functionalized surfaces and biomolecules including proteins can attach to each other by covalent coupling methods using a broad range of chemistries depending on the functionality of the modified surfaces. Accordingly, active groups on the functionalized supports and the amino acid residues of enzymes can form a covalent bond to immobilize biomolecules on the surfaces. Generally, enzyme leakage from the supports is prevented by the covalent immobilization, compared with other methods. Nonetheless, the development of new immobilization methods is required to control the positioning, orientation, and conformation of the immobilized biomolecules. Otherwise, the immobilized enzymes may lose their activity or be oriented with the active site to the surface [14, 15]. Among these carriers, nanomaterials, particularly nanoparticles, have proved to be unique immobilization supports regarding their exceptional features such as their distinguished high surface area. It can reduce the diffusional limitations encountered in conventional reaction systems and increase the enzyme loading per unit mass of support [6, 8, 15]. However, significant obstacles in the enzyme-catalyzed processes such as the enzyme separation from the reaction mixtures have limited the industrial applications of the immobilized enzyme onto the nanomaterials. In addition, enzyme leaching, low solubility, and enzyme immobilization efficiency have been reported as the main limitations in the previous literature [16, 17]. Development of an efficient method for biocatalyst recovery from the reaction mixtures has been much considered. Very recently, nano-sized magnetic particles have been widely employed for the immobilization of biomolecules as excellent support since they could be easily collected from the reaction medium by placing a strong magnet near the mixture [15, 18–20]. The ease of separation of magnetic nanoparticles (MNPs) with the help of a magnetic field along with their low toxicity made them as a promising carrier for biomolecules immobilization objects [16, 21]. In addition, surface modification and functionalization of MNPs can be easily done by treating them with different chemical groups to provide functional groups for covalent coupling, make them chemically stable and prevent their aggregation since these nanoparticles need to remain suspended in the aqueous solution and not form aggregate due to magnetic or van der Waals interactions [8, 19, 22]. As another advantage, MNPs can be separated from the media using an external magnetic field [20]. Over the years, a range of chemical and coupling agents such as 1-ethyl-3-(3-dimethylaminopropyl) carbodiimide hydrochloride (EDC), 3-aminopropyltrimethoxysilane (APTMS) and (3-aminopropyl) triethoxysilane (APTES) were used to functionalize magnetic nanoparticles and prepare them for enzyme immobilization purposes. Moreover, cross-linking agents have a direct influence on the operational stability and play a crucial role in enzyme attachment on the nanocarriers [23–26]. Among the conventional protein cross-linking reagents, glutaraldehyde has been preferred as the crosslinker due to its low production cost, ability to bind covalently with most of proteins, broad applicability and availability. However, glutaraldehyde possesses some intrinsic drawbacks and cannot be generally utilized as a crosslinker in different processes. In some cases, using glutaraldehyde as the crosslinker causes the formation of lumps of enzyme molecules which hinder the active sites [27]. Additionally, the adjacent bonds of aliphatic bonds formed by glutaraldehyde could induce poor electron conductivity [13]. Thus, other types of crosslinkers have received increasing attention recently as the potential activating agents for biomolecule immobilization purposes. Tyrosinase is a type three copper metalloenzyme with two copper ions and one of the most studied enzymes due to its wide application in pharmaceutical, wastewater treatment and food industries [28, 29]. This enzyme can be found in plants, insects, microorganism, and mammalians and is generally implicated in various biochemical processes. Two distinct oxidation pathways including the hydroxylation of monophenols to ortho-diphenols (cresolase activity or monophenolase) and the oxidation of ortho-diphenols to ortho-quinones (catecholase activity or diphenolase) are catalyzed by tyrosinase in the presence of oxygen [30, 31]. These ortho-quinones are highly unstable and characterized by their quick polymerization. There are two cupric ions and one oxygen molecule in the active pocket of this enzyme and different binuclear copper structures coexist with four oxidation states including deoxy, oxy, met and deact-tyrosinase. The oxidation of diphenols and monooxygenation of phenols are catalyzed by the oxy form which presents 15% of the native enzyme. The dominant form (the met form) is responsible for the diphenolase activity. The deoxy form can bind one molecule of oxygen with the regeneration of the oxy form. Finally, the hydroxylation of diphenols was done by the deact form (fourth oxidation state) and this minor pathway is known as the suicide inactivation of the enzyme. The monophenolase activity of the tyrosinase is specified by a lag timerequired to produce oxy form generated from the met form [32, 33].

Until now few studies have been reported in the literature concerning the efficient immobilization of tyrosinase on MNPs. However, the synthesis of solid nanocarriers modified with desired functional groups for the immobilization of tyrosinase with high stability and reusability is still a considerable challenge. Therefore, our previous works were aimed to focus on the immobilization of tyrosinase onto the modified magnetic nanoparticles using (3-aminopropyl) triethoxysilane as a silane coupling agent [34, 35]. In the current work to achieve high capacity, reusable, and operationally stable nano-biocatalyst, superparamagnetic nanoparticles were synthesized using *N*-[3 (trimethoxysilyl)propyl]ethylenediamine as a novel

modifying agent while cyanuric chloride was an activating agent. The functionalized particles were used for tyrosinase immobilization. After the characterization by EDX, VSM and TGA analyses, operational features of the nanobiocatalyst were investigated to find out the effectiveness of the immobilization procedure. The particles developed using the proposed chemicals bear an interesting engineered surface with the advantages of both siloxane and diamine groups, which can be exploited in broad applications such as biosensor development and wastewater treatment. Furthermore, the modifying agent in the current study is safe and inexpensive compared with (3-aminopropyl) triethoxysilane used for surface modification in our previous work.

Materials and methods

Materials

The edible mushroom (Agaricus bisporus) was obtained from the local market. *N*-[3-(trimethoxysilyl)propyl]ethylenediamine and L-dopa were acquired from Sigma-Aldrich. Tetrahydrofuran, Tetraethylorthosilicate (TEOS), Iron (III) chloride hexahydrate ($FeCl_3{\cdot}6H_2O$), ammonium sulfate, ethanol (99%), 2,4,6-Trichloro-1,3,5-triazine (cyanuric chloride), iron (II) chloride tetrahydrate ($FeCl_2{\cdot}4H_2O$), Coomassie brilliant blue G-250, Methanol (99.8%), Bovine serum albumin (BSA) and Ammonium hydroxide solution 25% were purchased from Merck. All other chemical reagents used in this study were analytical grade.

Synthesis of silica-coated magnetic nanoparticles

The Fe_3O_4 nanoparticles were synthesized and coated with silica according to the procedures reported before [34, 36]. Briefly, a mixture containing 300 mL of deionized water and 0.1 M solutions of $FeCl_3$ (100 mL) and $FeCl_2$ (50 mL) was prepared under a nitrogen atmosphere and its pH was adjusted using 1 M sodium hydroxide. Then, the mixture was mechanically stirred at 60 °C for 10 min and a strong magnet was used to separate the prepared magnetic nanoparticles. After washing with deionized water, the nanoparticles (560 mg) were added to 155 mL of ethanol and sonicated under a nitrogen atmosphere. 2000 µL of TEOS, 25 mL of deionized water and 12 mL of ammonium hydroxide solution were added to the mixture and stirred at room temperature for 5 h. Finally, the coated magnetic nanoparticles were separated using an external magnet, washed several times with ethanol, and deionized water.

Synthesis of functionalized iron oxide nanoparticles

The silica-coated magnetic nanoparticles were functionalized with an amino group using an adapted method [37]. For this purpose, 50 mL of methanol and 12.5 mL of *N*-[3-(trimethoxysilyl)propyl]ethylenediamine were added to 560 mg of the silica-coated magnetic nanoparticles and the suspension was agitated for 12 h and at 60 °C in a flask equipped with a mechanical stirrer. After that, the ethylenediamine functionalized magnetic nanoparticles (EMNPs) were collected by an external magnetic force, washed three times with tetrahydrofuran, and dried in a vacuum oven at 60 °C for 2 h. As the final step, the EMNPs were added to a mixture containing 50 mL of dry tetrahydrofuran and 0.25 g cyanuric chloride and the suspension was agitated for 3 h at 0 °C in water bath [38]. Then, the cyanuric chloride functionalized magnetic nanoparticles (Cyc-EMNPs) were separated, washed with tetrahydrofuran several times and dried under vacuum at 40 °C.

Immobilization of fresh enzyme onto the Cyc-MNPs

Tyrosinase was extracted from fresh mushroom and stored at − 22 °C [34, 39]. Then, 1.2 mL of phosphate buffer (pH 7.0 and 0.05 M) was added to the modified iron oxide nanoparticles (5 mg) and ultrasonicated for 40 s. Finally, 550 µL of the prepared tyrosinase solution was added to the suspension and shaken for 16 h at room temperature. At the end of the reaction, immobilized tyrosinase onto the modified magnetic nanoparticles (Ty-Cyc/EMNPs) was collected from the mixture by a magnet and washed with phosphate buffer to remove unbound enzyme. The activity of the free and immobilized enzyme was calculated based on the method described by Lu et al. with minor modification, using L-tyrosine (1 mM, pH 7.0) as the substrate [40]. Thus, 550 µL of L-tyrosine solution prepared in phosphate buffer (0.05 M and pH 7.0) was added to 16.7 µL of the free enzyme. Immediately, the mixture was transferred into a cuvette and the increase in absorbance was recorded spectrophotometrically at specified time intervals and 475 nm. To measure the activity of the immobilized tyrosinase, a proper amount of Ty-Cyc/EMNPs was added to 550 µL of L-tyrosine solution and the suspension was shaken. Then, the magnetic particles were separated from the mixture in 1 min intervals using a strong magnet. The absorbance of the supernatant at 475 nm was recorded. This appropriate amount of immobilized tyrosinase was chosen in such a way to maintain the absorbance of the reaction product within the linear range of the UV-spectrophotometer used in this work. The amount of enzyme causing an absorbance increase by 0.001/min at room temperature is described as the enzyme activity unit (U). The final and initial concentration of tyrosinase in the solution

used for immobilization was measured by the Bradford method using bovine serum albumin as standard to assay the amount of the enzyme attached to the Cyc/EMNPs [41]. In this regard, Eq. (1) was used to calculate the loading efficiency:

$$\text{Loading efficiency } (\%) = \left[\left(PC_i - PC_f\right)/PC_i\right] \times 100, \quad (1)$$

where PC_i is the initial amount of protein and PC_f is the amount of unbound enzyme collected after washing (three times) the immobilized tyrosinase with phosphate buffer solution.

Activity of Ty-Cyc/EMNPs and free tyrosinase at different operating conditions

The effect of different temperatures and pHs on the activity of free and immobilized tyrosinase was investigated. In this regard, L-tyrosine solution was prepared with different pHs (5.0–8.0) using phosphate and citrate phosphate buffer (0.05 M) to assay the activity of Ty-Cyc/EMNPs and free enzyme at room temperature. In addition, the activity of free and immobilized tyrosinase was determined at a temperature range of 15–55 °C using L-tyrosinase solution (pH 7.0) to investigate the effect of different temperatures on enzyme activity. The highest activities assayed at different temperatures and pHs were considered as 100% and other activities were represented relatively. Furthermore, the optimum condition for both immobilized and free tyrosinase was specified.

Stability of Ty-Cyc/EMNPs

For stability studies, a proper amount of immobilized tyrosinase was added to phosphate buffer or citrate phosphate buffer solution with different pH and temperature values. To examine the stability of Ty-Cyc/EMNPs in the pH range of 5.0–8.0, the suspensions containing immobilized tyrosinase and buffer solutions with different pHs were kept at room temperature for 2 h. Then, samples were taken and the activity of the immobilized tyrosinase was assayed at room temperature and pH 7.0. Similar experiments were conducted to investigate the thermal stability of Ty-Cyc/EMNPs. In this regard, the immobilized tyrosinase was incubated in phosphate buffer (pH 7.0 and 0.05 M) at different temperatures (15, 45, 55 and 65 °C) for 2 h and at known time intervals, and its activity was measured at room temperature. The activity of the immobilized tyrosinase at pH 7.0 and room temperature without incubating in the buffer solutions with different pHs and temperatures, was set as 100%.

Kinetic properties

A set of experiments were designed to determine the kinetic parameters of free and immobilized tyrosinase using the Michaelis–Menten model. Accordingly, L-dopa solution with different concentrations (0.5–5 mM) were prepared in phosphate buffer (pH 7.0) as the substrate, and the activity of tyrosinase was assayed at room temperature.

$$\upsilon = \frac{-d_s}{d_t} = \frac{\upsilon_{\max} S}{K_m + S}. \quad (2)$$

In Eq. (2), K_m, $\upsilon_{\max}$, and S are representing the Michaelis–Menten constant, the maximum rate of reaction and the concentration of L-dopa (the substrate) respectively. The graph of activity versus the L-dopa concentration was plotted to determine K_m and $\upsilon_{\max}$ as constants of the model. In this regard, non-linear fitting of the model to the data obtained from experiments was used to calculate the values of the constants ($\upsilon_{\max}$ and K_m).

Dephenolization capability of Ty-Cyc/EMNPs

20 mL of a phenol solution with a concentration of 100 ppm (pH 7.0) was added to 5 mg of Ty-Cyc/EMNPs and shaken for 2 h at room temperature. Samples were collected at 20 min intervals and the immobilized tyrosinase was magnetically separated from the suspension. The residual phenol concentration in the supernatants was measured colorimetrically at 510 nm by the method described in the previous works [42, 43]. 4-aminoantypyrine and potassium ferricyanide are the two chemical reagents used in this method.

Reusability of the immobilized enzyme

The Ty-Cyc/EMNPs were used in a different number of reaction cycles to determine their reusability at different temperature and pHs. An adequate amount of immobilized tyrosinase was added to 550 µL of L-tyrosinase prepared in phosphate buffer (pH 6.0, 7.0 and 8.0) or citrate phosphate buffer (pH 5.0) and the mixture was shaken. The activity of Ty-Cyc/EMNPs was assayed for each reaction cycle at room temperature. Magnetic nanoparticles carrying tyrosinase were collected from the mixture at the end of each cycle magnetically and washed (three times) with phosphate or citrate phosphate buffer. Then, the fresh substrate solution was added to the separated particles to start the next cycles. Furthermore, similar experiments were carried out at different temperatures (15–55 °C) and pH 7.0 to investigate the effect of temperature on the reusability of Ty-Cyc/EMNPs.

The highest activity measured in these tests was designated as 100%, and the other ones (at different temperatures and pHs) were reported relatively.

Effect of ultrasound on the immobilized enzyme activity

The effect of ultrasound waves on the activity of immobilized tyrosinase was investigated. For this purpose, L-tyrosine solution was added to the Ty-Cyc/EMNPs and the activities of all suspensions were measured after sonication for 1 min intervals at different frequencies (37 and 80 GHz) and power levels (30–100%). The experiments were conducted at room temperature and pH 7.0 and the activity of the immobilized tyrosinase without sonication was considered as 100%.

Characterization

The crystal structure and phase purity of the synthesized magnetic nanoparticles were determined by X-ray powder diffraction (XRD) (Bruker D8 Advance, with Cu Kα radiation, $\lambda = 0.154060$ nm) of the dried particles with scanning range from 4° to 70°. Scanning electron microscopy (SEM) equipped with Energy-dispersive X-ray (EDX) detector was used to characterize the morphological structure of magnetic nanoparticles and record EDX spectra of Ty-Cyc/EMNPs on a TESCAN Vega Model. Thermogravimetric analysis (TGA) was conducted on the dried particles, under a pure nitrogen atmosphere and a temperature range of 22–800 °C at a uniform heating rate of 10 °C (Netzsch – TGA 209F1). To analyze magnetization properties of the magnetic nanoparticles, a vibrating-sample magnetometer (VSM, Meghnatis Kavir Kashan Co., Iran) was used. The transmission electron microscopy (TEM) images were taken to study the size and morphology of the nanoparticles (using transmission electron microscopy operating at 220 kV). The Fourier transform Infrared (FTIR) Spectra of magnetic nanoparticles with different functional groups were acquired by FTIR analysis (PERKIN-ELMER).

Result and discussion

The functionalized magnetic nanoparticles characterization

X-Ray diffraction analysis

This analysis is a non-destructive technique generally used to investigate the crystalline properties and interlayer changes of the synthesized materials. As indicated in Fig. 1, five characteristic diffraction peaks ($2\theta = 30.07°$, 35.41°, 43.19°, 54.38°, 57.24°, and 62.83°) related to the corresponding indices of 220, 311, 400, 422, 511 and 440 were detected. According to the standard XRD cards of magnetic nanoparticles crystal (JCPDS No. 85-1436), it can be concluded that the synthesized iron oxide nanoparticles have a cubic spinel structure. In addition, the average size of the magnetic nanoparticles was calculated about 14 nm based on the Debye–Scherrer's equation [44].

SEM results of iron oxide nanoparticles

The SEM images of bare magnetic nanoparticles and Ty-Cyc/EMNPs were taken to investigate and visualize the surface morphology of the nanoparticles. To perform the SEM analysis, all samples were ultrasonicated for a defined time period for better dispersion. As illustrated in Fig. 2a and b, the differences between the surface structures of two samples could be observed and attributed to the surface modification

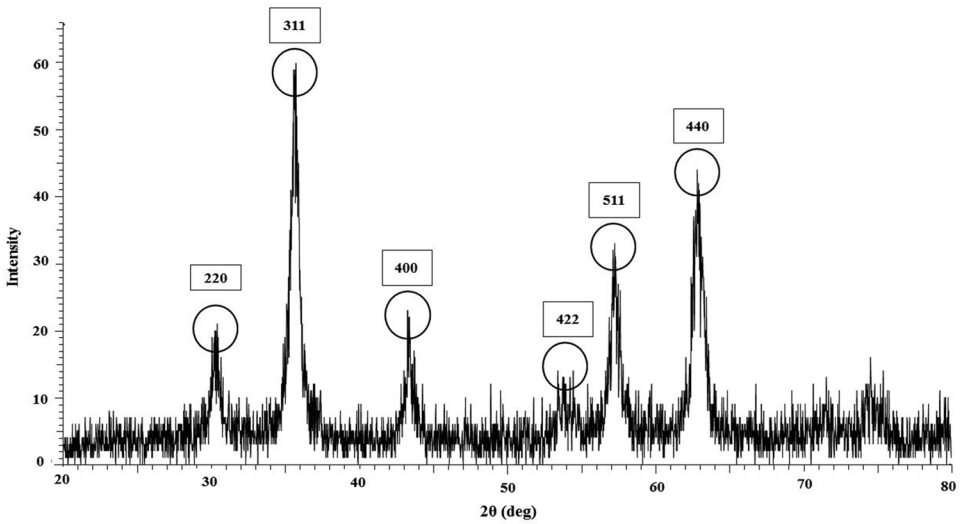

Fig. 1 XRD pattern of the Fe3O4 nanoparticles

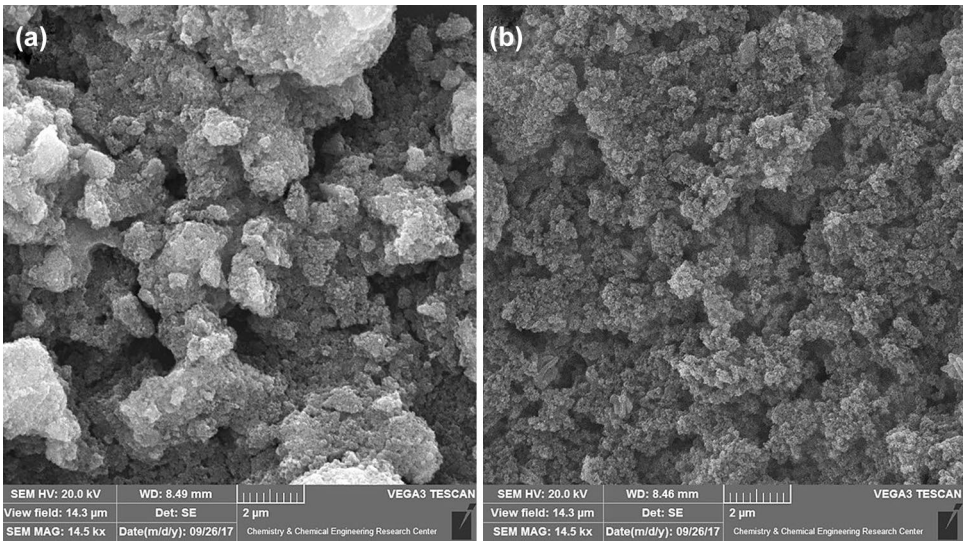

Fig. 2 Scanning electron microscopy of **a** bare MNPs and **b** Ty-Cyc/EMNPs

of iron oxide nanoparticles with the chemical groups and enzyme. In addition, the spherical shape of the nanoparticles and their small dimensions can be seen in this figure.

FTIR analysis of the nanoparticles

The Fourier transform infrared spectra of five samples (bare magnetic nanoparticles, silica-coated magnetic nanoparticles, Cyc/EMNPs, and Ty-Cyc/EMNPs) were recorded and used to screen the reactions (Fig. 3). For the bare

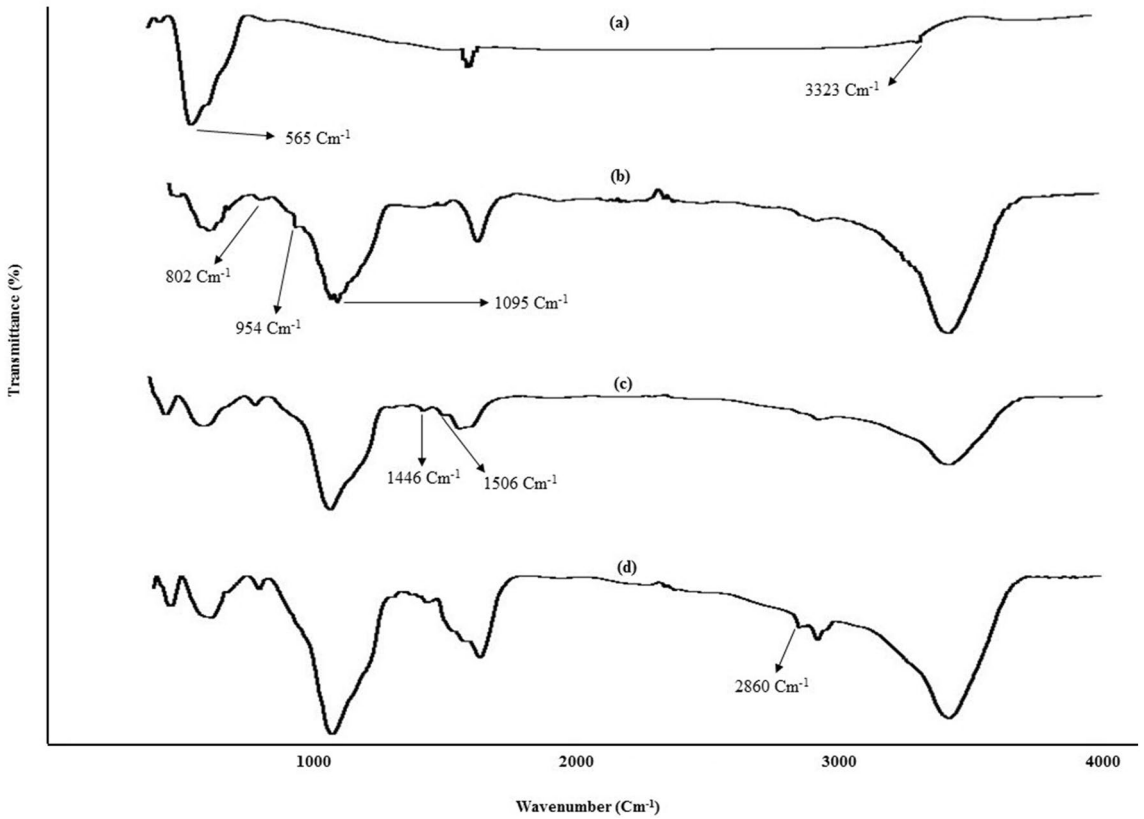

Fig. 3 FTIR spectra of **a** MNPs, **b** silica-coated MNPs, **c** Cyc/EMNPs and **d** immobilized tyrosinase

nanoparticles, the peaks at about 3323 cm^{-1} and 565 cm^{-1} are assigned to the H–O–H and Fe–O bonds, respectively [45]. Furthermore, two weak bands at 954 and 802 cm^{-1} in addition to a strong band at 1095 cm^{-1} were indicated in the FTIR spectra of silica-coated MNPs and corresponding to the vibrations of Si–O–Fe, Si–OH, and Si–O–Si, respectively [46]. There were two bands at 1446 and 1506 cm^{-1} in the spectrum of Cyc-MNPs demonstration the existence of cyanuric chloride components attached to the surface of the modified iron oxide nanoparticles. The appearance of a new characteristic band at 2860 cm^{-1} in the FTIR spectra of Ty-Cyc/EMNPs in comparison with the spectrum of cyanuric chloride modified nanoparticles, which is ascribed to the C-H aliph bond, supporting the successful attachment of tyrosinase onto the functionalized MNPs [38].

Vibrating-sample magnetometer (VSM) analysis results

The magnetization curves of the bare iron oxide nanoparticles, silica-coated magnetic nanoparticles, and Ty-Cyc/EMNPs were plotted to investigate the magnetic properties of samples (Fig. 4). Based on the results, all of the samples showed superparamagnetic behavior, and the saturation magnetization (Ms) values of Ty-Cyc/EMNPs, silica-coated magnetic nanoparticles, and bare Fe_3O_4 were 15.6, 24.6 and 45.9 emu/g, respectively. The reduction in Ms value of silica-coated Fe_3O_4 compared with the bare nanoparticles are due to the formation of silica coating over the surface of magnetic nanoparticles. Furthermore, the results indicated that the functionalization of MNPs and the enzyme immobilization caused the reduction of the magnetization properties as the Ms value of Ty-Cyc/EMNPs value was lower than the silica-coated nanoparticles.

In addition, the ease of separation of the Ty-Cyc/EMNPs was tested by dispersing the immobilized tyrosinase in an aqueous solution. An external magnet was placed near the suspension and it was observed that the Ty-Cyc/EMNPs were collected from the solution within 1 min. The result obtained from this experiment confirmed the good magnetic separation capability of the immobilized tyrosinase even with the reduction in its Ms value.

Thermogravimetric analysis

Further characterization of the Fe_3O_4 nanocarriers was carried out by TGA. In this regard, Cyc/EMNPs and Ty-Cyc/EMNPs were selected and their weight loss curves versus temperature were plotted. The weight loss step observed in the temperature range of 22–200 °C can be attributed to the removal of physically absorbed water molecules on the surface of nanoparticles. As shown in Fig. 5, the weight loss difference between the Cyc/EMNPs and Ty-Cyc/EMNPs in the second temperature range (200–800 °C) was about 13.54% and could correspond to the thermal decomposition of the immobilized enzyme. Consequently, the attachment of tyrosinase on the ethylenediamine functionalized iron oxide nanoparticles can be confirmed.

Transmission electron microscopy result of Ty-Cyc/EMNPs

TEM method was used to characterize the Ty-Cyc/EMNPs. As indicated in Fig. 6, the nanoparticles were successfully coated with the silica shell and had diameters in the nanometer range. The dark core shown in the TEM images corresponds to the magnetic nanoparticles and the light shell is related to the silica shell after the functionalization of MNPs. The results showed that Ty-Cyc/EMNPs had semispherical shapes. The larger specific area was provided by the small dimensions of the synthesized magnetic nanoparticles which resulted in higher enzyme immobilization.

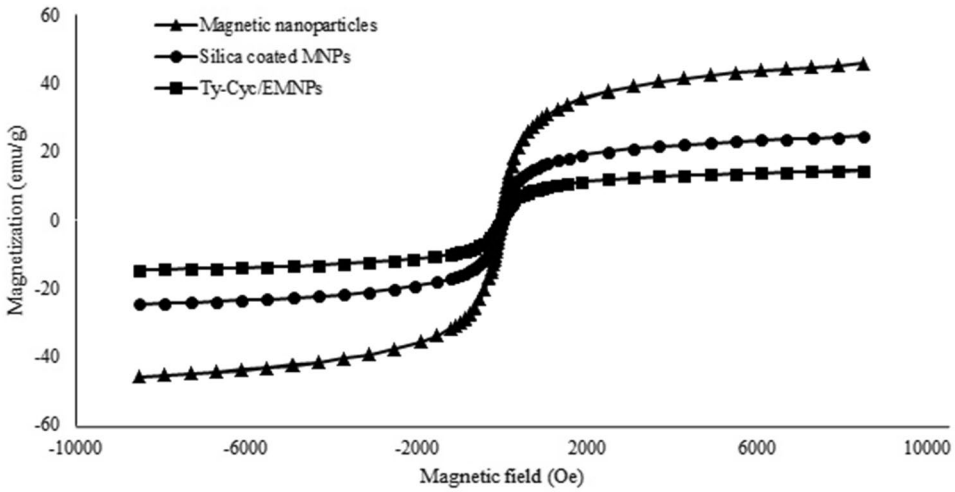

Fig. 4 Magnetization curves of **a** MNPs, **b** silica-coated Fe_3O_4 and **c** Ty-Cyc/EMNPs

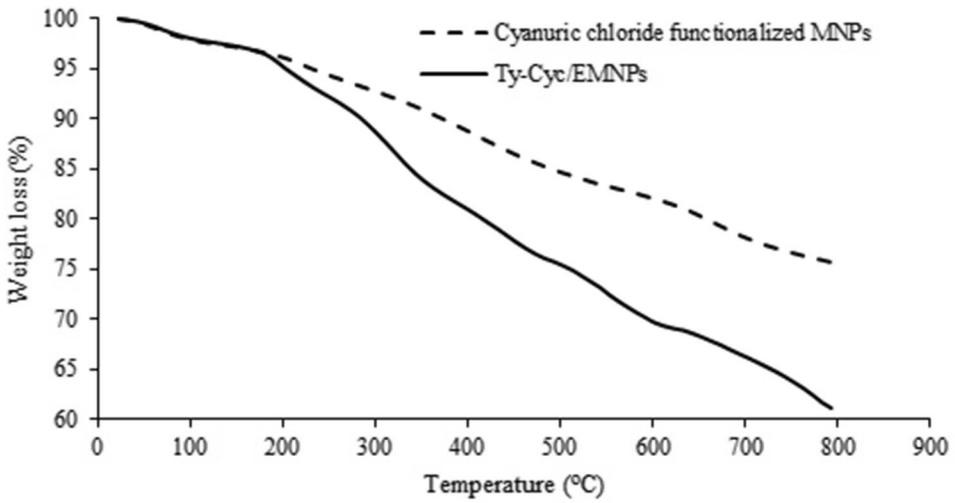

Fig. 5 Thermogravimetric analysis of **a** Cyc/EMNPs and **b** Ty-Cyc/EMNPs

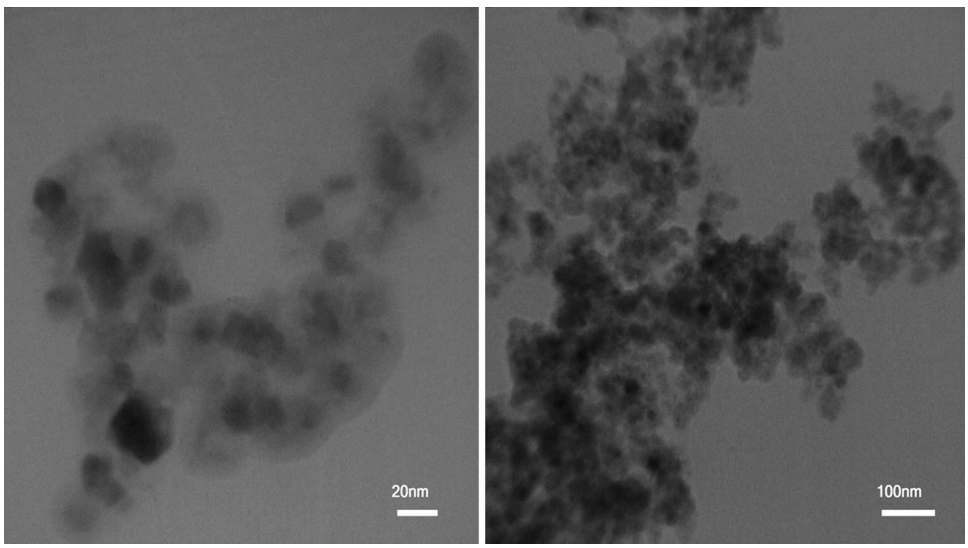

Fig. 6 Transmission electron microscopy images of Ty-Cyc/EMNPs

Energy-dispersive X-ray (EDX) spectrum

To confirm the attachment of tyrosinase to the functionalized MNPs, EDX analysis was performed and copper was detected in the spectrum of the Ty-Cyc/EMNPs (Fig. 7). As mentioned before, tyrosinase is known as a copper-containing enzyme and it could be concluded that tyrosinase was covalently immobilized onto the nanoparticles as other chemical agents used in this work do not contain copper.

Characterization of the Ty-Cyc/EMNPs

The activity of tyrosinase after extraction was greater than 12,000 U/mL. To conduct the experiments in this work, the extracted enzyme was diluted to 4500 U/mL using phosphate buffer. The average activity of the immobilized enzyme was calculated at about 151 U/g. The amount of immobilized enzyme onto the Cyc/EMNPs was compared with the values obtained from previous studies and the results are shown in Table 1. The higher enzyme loading capacity of the Cyc/EMNPs can be due to the high reactivity of the activating agent (cyanuric chloride) attached to the amine groups of the *N*-[3-(trimethoxysilyl)propyl]ethylenediamine as well as the large surface area of the nanoparticles. Moreover, the schematic illustration of the preparation of the Ty-Cyc/EMNPs is presented in Scheme 1.

Activity of free and immobilized tyrosinase at different pHs and temperatures

The activities of Ty-Cyc/EMNPs and free tyrosinase were affected by different temperatures (15–55 °C) and pHs (5.0–8.0). In this regard, the activities of the immobilized and free enzyme were compared with each other at different conditions. As shown in Fig. 8a, the highest activity of the immobilized and free tyrosinase were assayed at pH 7.0.

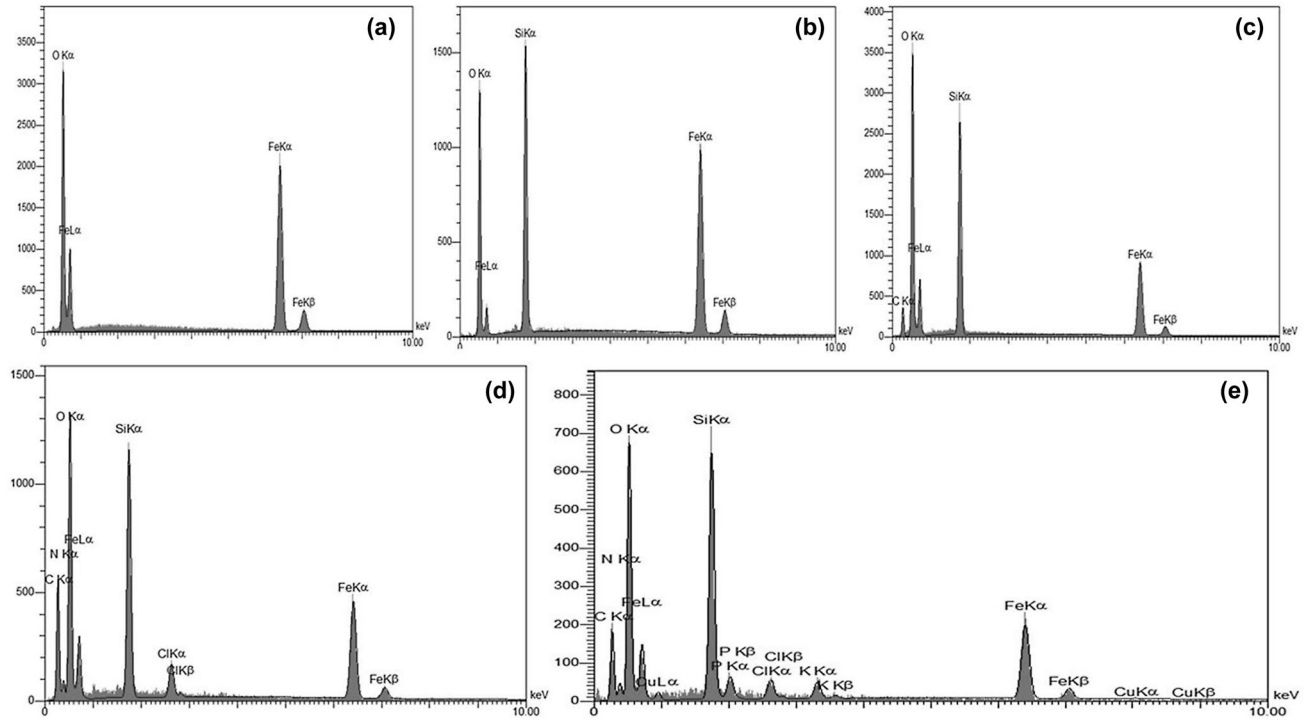

Fig. 7 EDX Spectrum of **a** bare MNPs, **b** silica-coated magnetic nanoparticles, **c** ethylenediamine functionalized Fe_3O_4-nanoparticles, **d** cyanuric chloride functionalized MNPs and **e** Ty-Cyc/EMNPs

Table 1 Enzyme loading capacity of various supports

Support	Enzyme	Enzyme loading (mg/g)	Reference
Polymethylchloride styrene	Tyrosinase	4.17	[47]
Ca-Alginate beads	Tyrosinase	2.26	[48]
Glass beads	Tyrosinase	1.18	[49]
SBA-15 mesoporous silica	Horseradish peroxidase	40	[50]
Magnetic beads	Tyrosinase	2.8	[51]
Polyurea microspheres	Laccase	20.63	[52]
Microperl industrial glass beads	Tyrosinase	1.18	[53]
Chitosan-Clay composite beads	Tyrosinase	26.8	[54]
PEGylated polyurethane nanoparticles	Horseradish peroxidase	25.5	[55]
Diatoms biosilica particles	Tyrosinase	37.1	[56]
Metal-ion-chelated magnetic microspheres	Laccase	100	[57]
Dry epoxy-silica	Tyrosinase	30.23	[58]
Cyc/EMNPs	Tyrosinase	123–132	This work

The activity of free and immobilized tyrosinase decreased at pH 5.0. This reduction in the relative activity of free and immobilized tyrosinase could be related to the net positive charge of the enzyme at this pH due to the tyrosinase isoelectric point (pI) (4.7) [59]. Moreover, the relative activities of the Ty-Cyc/EMNPs measured at pH 5.0 and 8.0 (58 and 72%, respectively) were higher than the values for the corresponding pHs in another research which has been conducted recently and focusing on the immobilization of tyrosinase on a membrane [60]. The effect of temperature on the activity of immobilized and free tyrosinase was indicated in Fig. 8b.

Both Ty-Cyc/EMNPs and the free enzyme had the highest activity at 35 °C. The relative activities of free and immobilized tyrosinase decreased as the temperature increased from 35 to 55 °C due to enzyme deactivation at these conditions. So, based on the results, it seems that the optimum condition

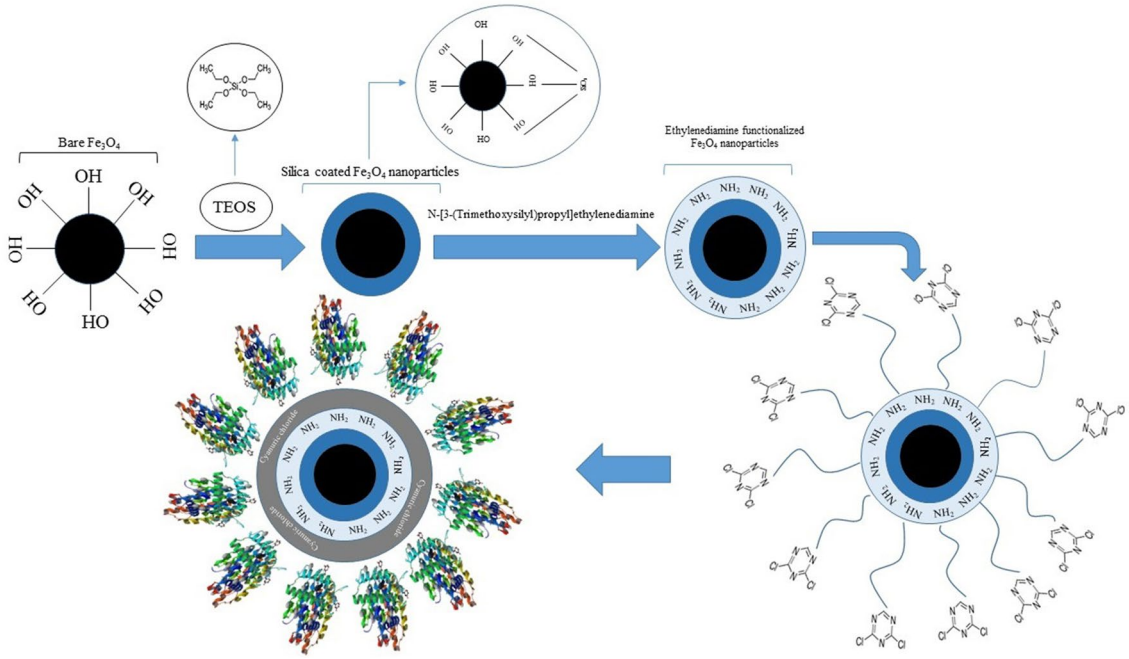

Scheme 1 Schematic representation of the procedure used for the preparation of the Ty-Cyc/EMNPs

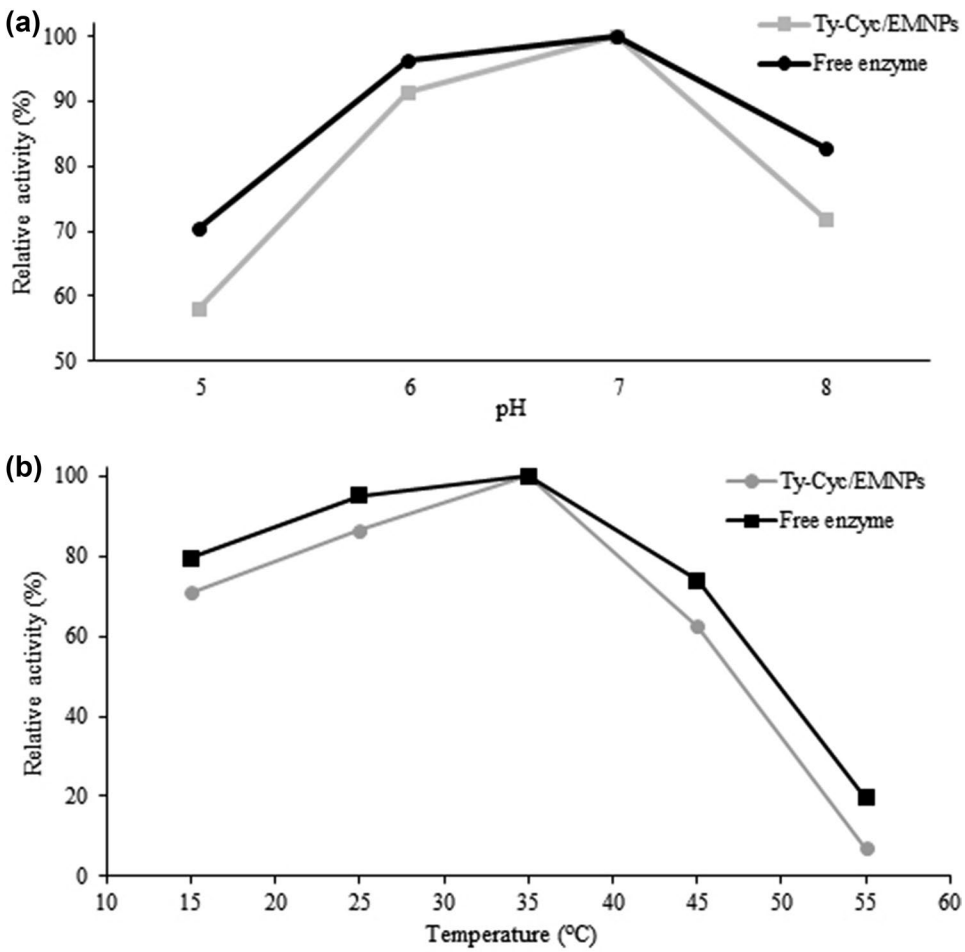

Fig. 8 Relative activity of the Ty-Cyc/EMNPs at different **a** pHs and **b** temperatures

for the immobilized and free tyrosinase was pH 7.0 and temperature 35 °C. The lower relative activities of the Ty-Cyc/EMNPs compared to the free enzyme could be attributed to the mass transfer limitations and immobilization process.

Stability of the immobilized enzyme

The stability of the Ty-Cyc/EMNPs was evaluated at various temperatures and pHs. As indicated in Fig. 9a, more than 65% of the activity of the immobilized tyrosinase was retained after 2 h incubation at pH 5.0.

In addition, the immobilized tyrosinase was stable for 60 min at pH 8.0 and its relative activity was measured about 89%. Temperature is another parameter affects the stability of the immobilized tyrosinase and needs to be investigated. The relative activity of the Ty-Cyc/EMNPs reached 79% after incubation at 45 °C for 60 min (Fig. 9b). Moreover, no remarkable loss of activity (less than 8%) was observed after 120 min suspension at 15 °C. However, at 65 °C, the Ty-Cyc/EMNPs had almost no activity after 120 min incubation. It could be due to the thermal deactivation of tyrosinase at high temperatures. The considerable stability of Ty-Cyc/EMNPs was confirmed by the results obtained in this study. Enzyme immobilization on suitable carriers using appropriate techniques can cause an increase in the conformational rigidity of enzyme structure and limit its sensitivity to severe conformational changes [61].

Kinetic results

Changes in the Michaelis–Menten constant (K_m) and maximum rate of the reaction (υ_{max}) of tyrosinase due to immobilization were investigated to monitor the success of the immobilization procedure used in this work. For this purpose, the Michaelis–Menten model was fitted to the corresponding data obtained in this set of experiments as shown in Fig. 10a and b. Based on the calculation, the υ_{max} and K_m values were 20,063 U/mg protein and 5.02 mM for the Ty-Cyc/EMNPs and 27,242 U/mg protein and 1.49 mM for free tyrosinase, respectively.

The results showed that the immobilized tyrosinase has a lower affinity for the substrates compared to the free

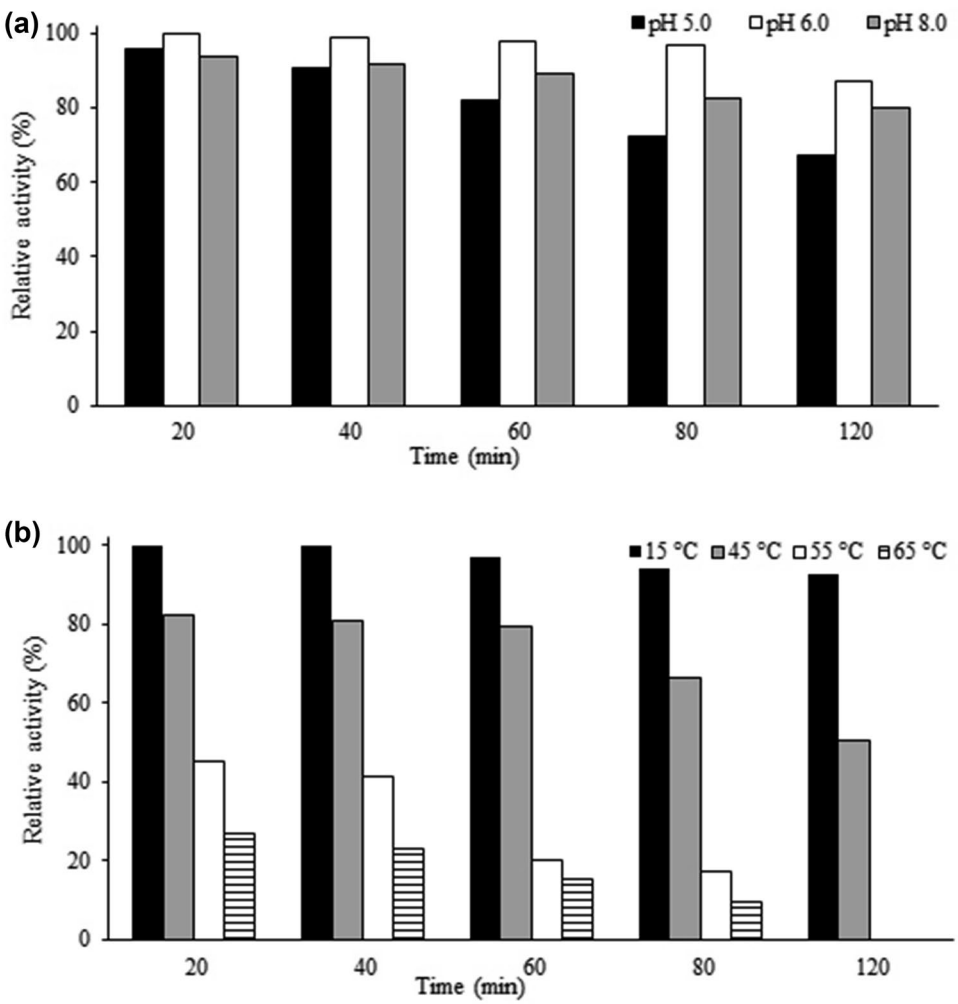

Fig. 9 Effect of different **a** pHs and **b** temperatures on the stability of the Ty-Cyc/EMNPs

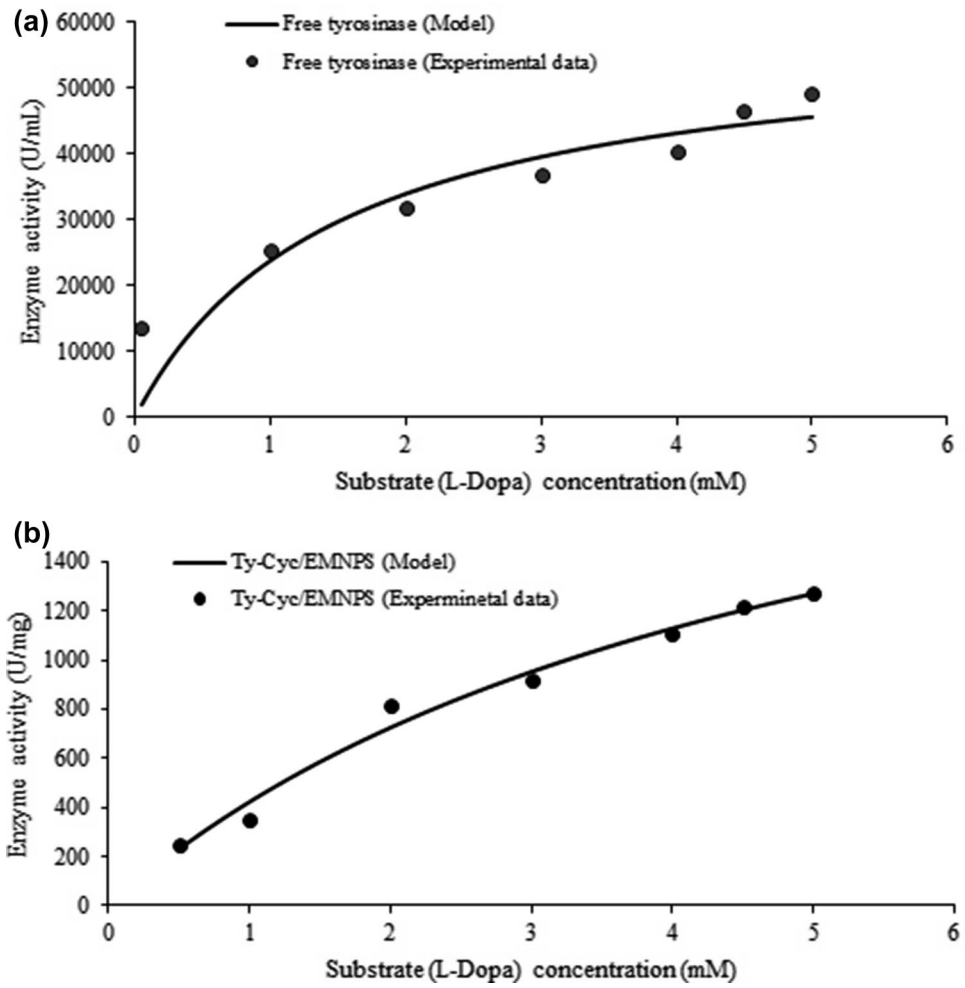

Fig. 10 Michaelis-Menten curves for the **a** free tyrosinase and **b** Ty-Cyc/EMNPs using different substrate concentration

enzyme since its K_m value was higher than that for the free one. This can be justified by the inherent properties of immobilization processes. The diffusional limitations and enzyme structural changes during the immobilization are responsible for the differences between the affinities of the immobilized and free tyrosinase during the immobilization. Moreover, the introduction of steric hindrance constituted by the carrier toward the active site of enzymes resulting in the lack of sufficient enzyme flexibility for binding of the natural ligands during catalysis is known as another parameter which effects on the affinities of the free and immobilized enzymes.

Furthermore, the obtained υ_{max} value for the Ty-Cyc/EMNPs was higher than those from the recent studies (18.61 U/g [56, 62] and 19.8 U/mg protein) which could be due to the high amount of active enzyme attached to the carrier as the Cyc/EMNPs is highly reactive and have a large surface area as confirmed before. As a result, the kinetic parameters can be enhanced by immobilization using the procedure employed in this work.

Phenol removal by the Ty-Cyc/EMNPs

The ability of a small portion of the immobilized tyrosinase to remove phenolic compounds from aqueous solutions was evaluated using a phenol solution with a concentration of 100 mg/mL at room temperature and pH 7.0. As illustrated in Fig. 11, Ty-Cyc/EMNPs degraded more than 75% of

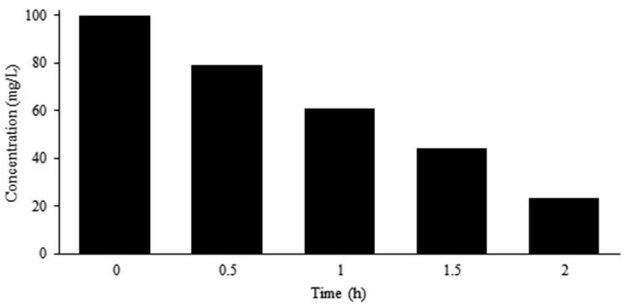

Fig. 11 Enzymatic removal of phenol from an aqueous solution (100 mg/L) by the Ty-Cyc/EMNPs

phenol in 2 h and the results show the considerable potential of the prepared nano-biocatalyst for wastewater treatment.

Reusability of the Ty-Cyc/EMNPs

The reusability and recoverability of the immobilized tyrosinase can be improved by the incorporation of enzyme immobilization and magnetic technology. The activity of the Ty-Cyc/EMNP was assayed after repeated runs to investigate its reusability. The immobilized tyrosinase retained more than 50% of its initial activity after reusing for six cycles at pH 7.0 and the data was shown in Fig. 12a. Furthermore, less than 7% activity loss occurred for the Ty-Cyc/EMNPs in the first three cycles at room temperature and pH 7.0. The relative activity of the immobilized tyrosinase after the third reaction cycle at pH 5.0 was measured about 36%. This significant reduction in the relative activity of the Ty-Cyc/EMNPs could be due to the pI point of tyrosinase which discussed before. Generally, the main reason for the activity loss could be the recurrent encountering of the active site of Ty-Cyc/EMNP and substrate which resulted in its distortion and loss of activity. The immobilized enzyme had a good performance in several reaction cycles at different temperatures so that about 53% of its initial activity remained after reused for five cycles (Fig. 12b). However, the relative activity of Ty-Cyc/EMNPs was decreased to below 30% after the fourth cycle at 45 °C. This activity loss might be attributed to the enzyme deactivation at high temperatures and under harsh conditions. These data confirmed that the Ty-Cyc/EMNPs could be employed in multiple reaction cycles with adequate levels of activity.

Ultrasonic waves

The suspension of Ty-Cyc/EMNPs and L-tyrosine solution was ultrasonicated to evaluate the influence of ultrasound waves on their activities. The immobilized tyrosinase had a higher activity after using ultrasound compared to the activity of the Ty-Cyc/EMNPs measured without applying the ultrasound. It might be related to an increase in the internal energy of the substrate due to the use of ultrasound and better dispersion of the magnetic nanoparticles in the substrate solution which increased the likelihood of the enzyme–substrate combinations. Moreover, in some cases, it has been

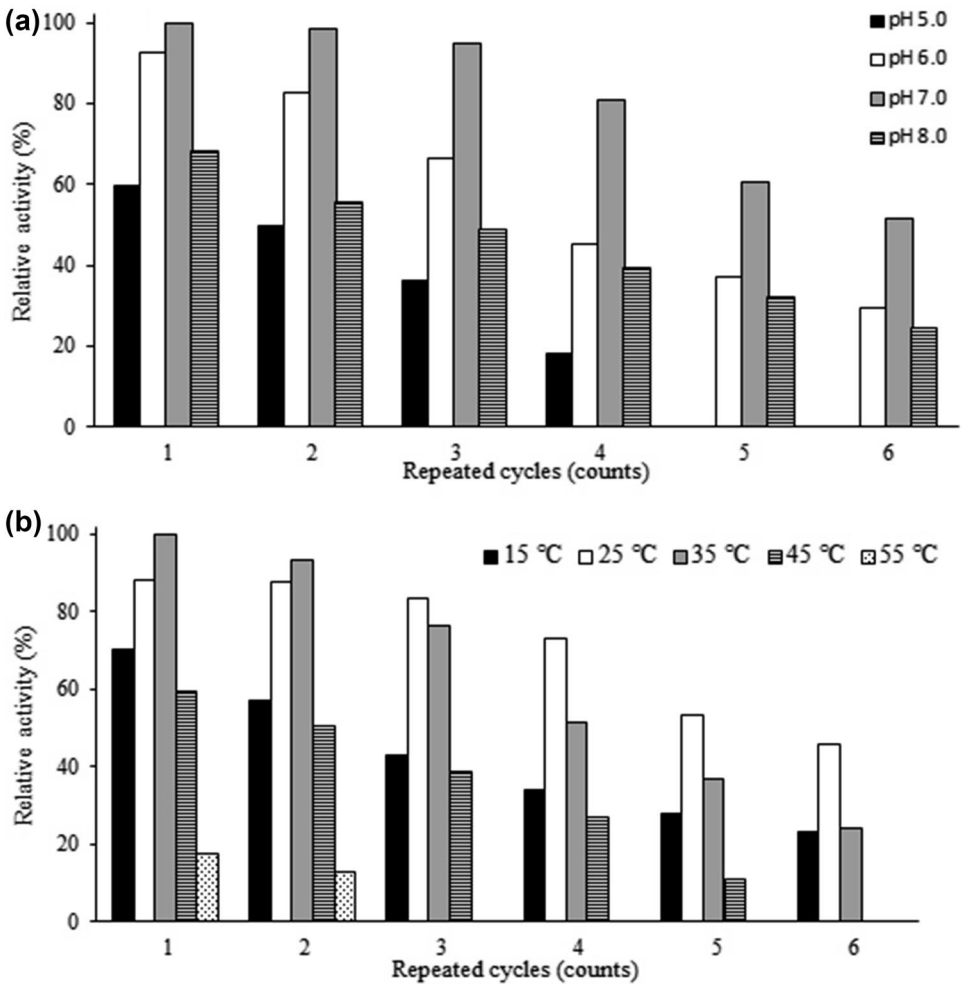

Fig. 12 Reusability of the Ty-Cyc/EMNPs at different **a** pH values and **b** temperatures

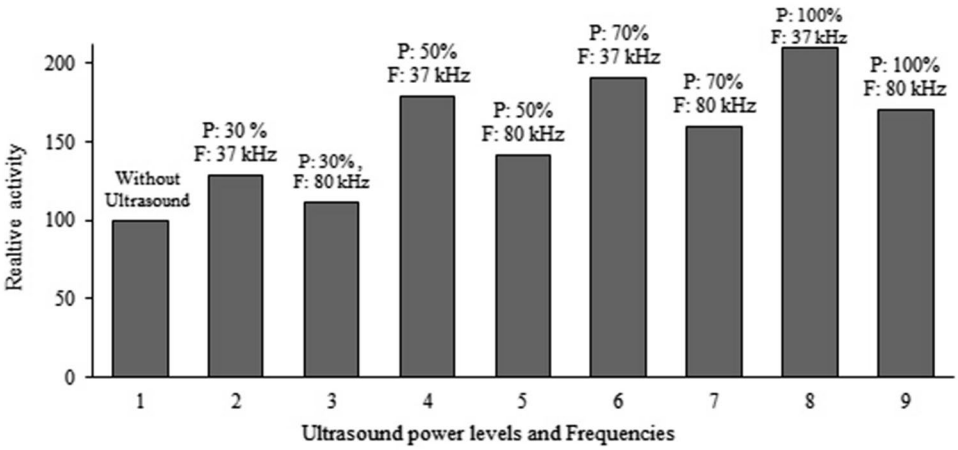

Fig. 13 Effect of ultrasonic waves on the activity of the immobilized tyrosinase

reported that the monophenolase and diphenolase activities of several enzymes, such as laccase, alcohol dehydrogenase, protease, and lipase can be affected by ultrasound. It can be because of the enhancement of mass transfer due to micromixing and enzyme release due to cell break-up [63]. As shown in Fig. 13, the activity change of the immobilized tyrosinase with ultrasound treatment (power 100% and 37 GHz) was more than 209% in comparison to the activity of Ty-Cyc/EMNPs assayed without using ultrasonic waves.

Conclusion

In this study, a robust and convenient nano-biocatalyst was fabricated by synthesizing a novel functionalized magnetic nanoparticle and using an inexpensive procedure. Incorporating the benefits of easy separation and particular physical features of the modified iron oxide, the Cyc/EMNPs were used for tyrosinase immobilization as an effective nano-biocatalyst. Covalent attachment of tyrosinase onto the functionalized nanoparticles was examined by EDX, VSM and TGA analyses. The highest catalytic activity of the Ty-Cyc/EMNPs was obtained at 35 °C and pH 7.0. The immobilized tyrosinase exhibited excellent stability at various pHs and temperatures. Furthermore, Ty-Cyc/EMNPs had a noticeable performance in repeated reaction cycles as if no significant loss of activity was observed in the first three cycles, although 50% of their initial activity remained after six cycles. The results prove that the use of *N*-[3-(trimethoxysilyl)propyl]ethylenediamine and cyanuric chloride for surface functionalization creates a new way of developing such efficient catalysts. The use of Cyc/EMNPs is promising to be expanded to the other enzyme systems. This magnetic nano-biocatalyst with fascinating properties, such as its high stability, reusability, and loading capacity, provides great opportunities for its practical applications in biotechnology, biosensor development, and wastewater treatment.

References

1. Choi J, Han S, Kim H (2015) Industrial applications of enzyme biocatalysis: current status and future aspects. Biotechnol Adv 33:1443–1454
2. Madhavan A, Sindhu R, Binod P, Sukumaran RK, Pandey A (2017) Strategies for design of improved biocatalysts for industrial applications. Bioresour Technol 245:1304–1313
3. Das R, Talat M, Srivastava ON, Kayastha AM (2018) Covalent immobilization of peanut β-amylase for producing industrial nano-biocatalysts: a comparative study of kinetics, stability and reusability of the immobilized enzyme. Food Chem 245:488–499
4. Das R, Mishra H, Srivastava A, Kayastha AM (2017) Covalent immobilization of β-amylase onto functionalized molybdenum sulfide nanosheets, its kinetics and stability studies: a gateway to boost enzyme application. Chem Eng J 328:215–227
5. Du Y, Gao J, Zhou L, Ma L, He Y, Huang Z, Jiang Y (2017) Enzyme nanocapsules armored by metal-organic frameworks: a novel approach for preparing nanobiocatalyst. Chem Eng J 327:1192–1197
6. Liu S, Höldrich M, Sievers-Engler A, Horak J, Lämmerhofer M (2017) Papain-functionalized gold nanoparticles as heterogeneous biocatalyst for bioanalysis and biopharmaceuticals analysis. Anal Chim Acta 963:33–43
7. Ji C, Nguyen LN, Hou J, Hai FI, Chen V (2017) Direct immobilization of laccase on titania nanoparticles from crude enzyme extracts of *P. ostreatus* culture for micro-pollutant degradation. Sep Purif Technol 178:215–223
8. Khan M, Husain Q, Bushra R (2017) Immobilization of β-galactosidase on surface modified cobalt/multiwalled carbon nanotube nanocomposite improves enzyme stability and resistance to inhibitor. Int J Biol Macromol 105:693–701
9. Wahba MI (2017) Porous chitosan beads of superior mechanical properties for the covalent immobilization of enzymes. Int J Biol Macromol 105:894–904
10. Tacias-Pascacio VG, Virgen-Ortíz JJ, Jiménez-Pérez M, Yates M, Torrestiana-Sanchez B, Rosales-Quintero A, Fernandez-Lafuente R (2017) Evaluation of different lipase biocatalysts in the production of biodiesel from used cooking oil: critical role of the immobilization support. Fuel 200:1–10

11. Schöffer JDN, Matte CR, Charqueiro DS, de Menezes EW, Costa TMH, Benvenutti EV, Rodrigues RC, Hertz PF (2017) Directed immobilization of CGTase: the effect of the enzyme orientation on the enzyme activity and its use in packed-bed reactor for continuous production of cyclodextrins. Process Biochem 58:120–127
12. Altinkaynak C, Tavlasoglu S, Özdemir N, Ocsoy I (2016) A new generation approach in enzyme immobilization: organic-inorganic hybrid nanoflowers with enhanced catalytic activity and stability. Enzyme Microb Technol 93–94:105–112
13. Chung Y, Christwardana M, Tannia DC, Kim KJ, Kwon Y (2017) Biocatalyst including porous enzyme cluster composite immobilized by two-step crosslinking and its utilization as enzymatic biofuel cell. J Power Sources 360:172–179
14. Khaldi K, Sam S, Lounas A, Yaddaden C, Gabouze N (2017) Comparative investigation of two methods for Acetylcholinesterase enzyme immobilization on modified porous silicon. Appl Surf Sci 421:148–154
15. Zhang Q, Kang J, Yang B, Zhao L, Hou Z, Tang B (2016) Immobilized cellulase on Fe_3O_4 nanoparticles as a magnetically recoverable biocatalyst for the decomposition of corncob. Chin J Catal 37:389–397
16. Khoshnevisan K, Vakhshiteh F, Barkhi M, Baharifar H, Poor-Akbar E, Zari N, Stamatis H, Bordbar A (2017) Immobilization of cellulase enzyme onto magnetic nanoparticles: applications and recent advances. Mol Catal 442:66–73
17. Landarani-Isfahani A, Taheri-Kafrani A, Amini M, Mirkhani V, Moghadam M, Soozanipour A, Razmjou A (2015) Xylanase immobilized on novel multifunctional hyperbranched polyglycerol-grafted magnetic nanoparticles: an efficient and robust biocatalyst. Langmuir 31:9219–9227
18. Sánchez-Ramírez J, Martínez-Hernández JL, Segura-Ceniceros P, López G, Saade H, Medina-Morales MA, Ramos-González R, Aguilar CN, Ilyina A (2017) Cellulases immobilization on chitosan-coated magnetic nanoparticles: application for *Agave Atrovirens* lignocellulosic biomass hydrolysis. Bioprocess Biosyst Eng 40:9–22
19. Xie W, Zang X (2017) Covalent immobilization of lipase onto aminopropyl-functionalized hydroxyapatite-encapsulated-γ-Fe_2O_3 nanoparticles: a magnetic biocatalyst for interesterification of soybean oil. Food Chem 227:397–403
20. Bezerra RM, Neto DMA, Galvão WS, Rios NS, Carvalho ACLM, Correa MA, Bohn F, Fernandez-Lafuente R, Fechine PBA, de Mattos MC, dos Santos JCS, Gonçalves LRB (2017) Design of a lipase-nano particle biocatalysts and its use in the kinetic resolution of medicament precursors. Biochem Eng J 125:104–115
21. Long J, Li X, Wu Z, Xu E, Xu X, Jin Z, Jiao A (2015) Immobilization of pullulanase onto activated magnetic chitosan/Fe_3O_4 nanoparticles prepared by in situ mineralization and effect of surface functional groups on the stability. Coll Surf Physicochem Eng Asp 472:69–77
22. Wang L, Chen G, Zhao J, Cai N (2017) Catalase immobilization on amino-activated Fe_3O_4@SiO_2 nanoparticles: loading density affected activity recovery of catalase. J Mol Catal B Enzym. https://doi.org/10.1016/j.molcatb.2017.03.011
23. Das A, Singh J, Yogalakshmi KN (2017) Laccase immobilized magnetic iron nanoparticles: fabrication and its performance evaluation in chlorpyrifos degradation. Int Biodeterior Biodegrad 117:183–189
24. Rouhani S, Rostami A, Salimi A (2016) Preparation and characterization of laccases immobilized on magnetic nanoparticles and their application as a recyclable nanobiocatalyst for the aerobic oxidation of alcohols in the presence of TEMPO. RSC Adv 6:26709–26718
25. Feng J, Yu S, Li J, Mo T, Li P (2016) Enhancement of the catalytic activity and stability of immobilized aminoacylase using modified magnetic Fe_3O_4 nanoparticles. Chem Eng J 286:216–222
26. Fortes CCS, Daniel-da-silva AL, Xavier AMRB, Tavares APM (2017) Optimization of enzyme immobilization on functionalized magnetic nanoparticles for laccase biocatalytic reactions. Chem Eng Process Process Intensif 117:1–8
27. Sojitra UV, Nadar SS, Rathod VK (2017) Immobilization of pectinase onto chitosan magnetic nanoparticles by macromolecular cross-linker. Carbohydr Polym 157:677–685
28. Guan Y, Liu L, Chen C, Kang X, Xie Q (2016) Effective immobilization of tyrosinase via enzyme catalytic polymerization of L-DOPA for highly sensitive phenol and atrazine sensing. Talanta 160:125–132
29. Chaves OA, de Barros LS, de Oliveira MCC, Sant'Anna CMR, Ferreira ABB, da Silva FA, Cesarin-Sobrinho D, Netto-Ferreira JC (2017) Biological interactions of fluorinated chalcones: stimulation of tyrosinase activity and binding to bovine serum albumin. J Fluor Chem 199:30–38
30. Soltani-Firooz N, Panahi R, Mokhtarani B, Yazdani F (2017) Direct introduction of amine groups into cellulosic paper for covalent immobilization of tyrosinase: support characterization and enzyme properties. Cellulose 24:1407–1416
31. Oyama T, Yoshimori A, Takahashi S, Yamamoto T, Sato A, Kamiya T, Abe H, Abe T, Tanuma S (2017) Structural insight into the active site of mushroom tyrosinase using phenylbenzoic acid derivatives. Bioorg Med Chem Lett 27:2868–2872
32. Vandeput M, Patris S, Silva H, Parsajoo C, Dejaeghere B, Martinez JA, Kauffmann JM (2017) Application of a tyrosinase microreactor–detector in a flow injection configuration for the determination of affinity and dynamics of inhibitor binding. Sensors Actuators B Chem 248:385–394
33. Labus K, Turek A, Liesiene J, Bryjak J (2011) Efficient Agaricus bisporus tyrosinase immobilization on cellulose-based carriers. Biochem Eng J 56:232–240
34. Abdollahi K, Yazdani F, Panahi R (2017) Covalent immobilization of tyrosinase onto cyanuric chloride crosslinked amine-functionalized superparamagnetic nanoparticles: synthesis and characterization of the recyclable nanobiocatalyst. Int J Biol Macromol 94:396–405
35. Abdollahi K, Yazdani F, Panahi R (2016) Data in support of covalent attachment of tyrosinase onto cyanuric chloride crosslinked magnetic nanoparticles. Data in Brief 9:1098–1104
36. Ranjbakhsh E, Bordbar AK, Abbasi M, Khosropour AR, Shams E (2012) Enhancement of stability and catalytic activity of immobilized lipase onsilica-coated modified magnetite nanoparticles. Chem Eng J 179:272–276
37. Ozdemir C, Akca O, Medine EI, Demirkol DO, Unak P, Timur S (2012) Biosensing applications of modified core–shell magnetic nanoparticles. Food Anal Methods 5(4):731–736
38. Soozanipour A, Taheri-kafrani A, Isfahani AL (2015) Covalent attachment of xylanase on functionalized magnetic nanoparticles and determination of its activity and stability. Chem Eng J 270:235–243
39. Zynek K, Bryjak J, Polakovič M (2010) Effect of separation on thermal stability of tyrosinase from *Agaricus bisporus*. J Mol Catal B Enzym 66(1–2):172–176
40. Lu L, Zhao M, Wang Y (2007) Immobilization of laccase by alginate–chitosan microcapsules and its use in dye decolorization. World J Microbiol Biotechnol 23(2):159–166
41. Bradford MM (1976) A rapid and sensitive method for the quantitation microgram quantities of protein utilizing the principle of protein-dye binding. Anal Biochem 72(1–2):248–254
42. Abdollahi K, Yazdani F, Panahi R, Mokhtarani B (2018) Biotransformation of phenol in synthetic wastewater using the functionalized magnetic nano-biocatalyst particles carrying tyrosinase. 3 Biotech 8(10):419

43. Alver E, Metin AÜ (2017) Chitosan based metal-chelated copolymer nanoparticles: laccase immobilization and phenol degradation studies. Int Biodeterior Biodegrad 125:235–242
44. Gautam RK, Gautam PK, Banerjee S, Soni S, Singh SK, Chattopadhyaya MC (2015) Removal of Ni(II) by magnetic nanoparticles. J Mol Liq 204:60–69
45. Veisi H, Gholami J, Ueda H, Mohammadi P, Noroozi M (2015) Magnetically palladium catalyst stabilized by diaminoglyoxime-functionalized magnetic Fe_3O_4 nanoparticles as active and reusable catalyst for Suzuki coupling reactions. J Mol Catal A Chem 396:216–223
46. Chen Y, Xiong Z, Zhang L, Zhao J, Zhang Q, Peng L, Zhang W, Ye M, Zou H (2015) Facile synthesis of zwitterionic polymer-coated core-shell magnetic nanoparticles for highly specific capture of N-linked glycopeptides. Nanoscale 7(7):3100–3108
47. Ho PY, Chiou MS, Chao AC (2003) Production of L-DOPA by tyrosinase immobilized on modified polystyrene. Appl Biochem Biotechnol 111(3):139–152
48. Yahşi A, Şahin F, Demirel G, Tümtürk H (2005) Binary immobilization of tyrosinase by using alginate gel beads and poly(acrylamide-co-acrylic acid) hydrogels. Int J Biol Macromol 36(4):253–258
49. Marín-Zamora ME, Rojas-Melgarejo F, García-Cánovas F, García-Ruiz PA (2007) Effects of the immobilization supports on the catalytic properties of immobilized mushroom tyrosinase: a comparative study using several substrates. J Biotechnol 131(4):388–396
50. Pitzalis F, Monduzzi M, Salis A (2017) A bienzymatic biocatalyst constituted by glucose oxidase and Horseradish peroxidase immobilized on ordered mesoporous silica. Microporous Mesoporous Mater 241:145–154
51. Tuncagil S, Kayahan SK, Bayramoglu G, Arica MY, Toppare L (2009) L-Dopa synthesis using tyrosinase immobilized on magnetic beads. J Mol Catal B Enzym 58(1–4):187–193
52. Jiang X, Yu Y, Li X, Kong XZ (2017) High yield preparation of uniform polyurea microspheres through precipitation polymerization and their application as laccase immobilization support. Chem Eng J 328:1043–1050
53. Marín-Zamora ME, Rojas-Melgarejo F, García-Cánovas F, García-Ruiz PA (2009) Production of *o*-diphenols by immobilized mushroom tyrosinase. J Biotechnol 139(2):163–168
54. Dinçer A, Becerik S, Aydemir T (2012) Immobilization of tyrosinase on chitosan–clay composite beads. Int J Biol Macromol 50(3):815–820
55. Fritzen-Garcia MB, Monteiro FF, Cristofolini T, Acuña JJS, Zanetti-Ramos BG, Oliveira IRWZ, Soldi V, Pasa AA, Creczynski-Pasa TB (2013) Characterization of horseradish peroxidase immobilized on PEGylated polyurethane nanoparticles and its application for dopamine detection. Sensors Actuators B Chem 182:264–272
56. Bayramoglu G, Akbulut A, Arica MY (2013) Immobilization of tyrosinase on modified diatom biosilica: enzymatic removal of phenolic compounds from aqueous solution. J Hazard Mater 244–245:528–536
57. Lin J, Liu Y, Chen S, Le X, Zhou X, Zhao Z, Ou Y, Yang J (2016) Reversible immobilization of laccase onto metal-ion-chelated magnetic microspheres for bisphenol A removal. Int J Biol Macromol 84:189–199
58. de Oliveira KB, Mischiatti KL, Fontana JD, de Oliveira BH (2014) Tyrosinase immobilized enzyme reactor: development and evaluation. J Chromatogr B 945–946:10–16
59. Rijiravanich P, Aoki K, Chen J, Surareungchai W, Somasundrum M (2006) Micro-cylinder biosensors for phenol and catechol based on layer-by-layer immobilization of tyrosinase on latex particles: theory and experiment. J Electroanal Chem 589(2):249–258
60. Donato L, Algieri C, Rizzi A, Giorno L (2014) Kinetic study of tyrosinase immobilized on polymeric membrane. J Memb Sci 454:346–350
61. Homaei AA, Sajedi RH, Sariri R, Seyfzadeh S, Stevanato R (2010) Cysteine enhances activity and stability of immobilized papain. Amino Acids 38(3):937–942
62. Wu Q, Xu Z, Duan Y, Zhu Y, Ou M, Xu X (2017) Immobilization of tyrosinase on polyacrylonitrile beads: biodegradation of phenol from aqueous solution and the relevant cytotoxicity assessment. RSC Adv 7(45):28114–28123
63. Yu Z-L, Zeng W-C, Lu X-L (2013) Influence of ultrasound to the activity of tyrosinase. Ultrason Sonochem 20(3):805–809